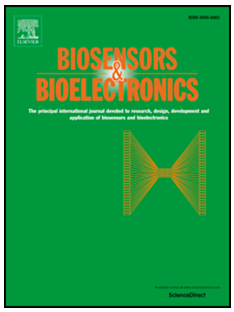

SERS-based immunoassay for monitoring cortisol-related disorders

Javier E.L. Villa, Isabel Garcia, Dorleta Jimenez de Aberasturi, Valeri Pavlov, Maria D.P.T. Sotomayor, Luis M. Liz-Marzán

PII: S0956-5663(20)30412-7

DOI: https://doi.org/10.1016/j.bios.2020.112418

Reference: BIOS 112418

To appear in: *Biosensors and Bioelectronics*

Received Date: 14 May 2020

Revised Date: 25 June 2020

Accepted Date: 29 June 2020

Please cite this article as: Villa, J.E.L., Garcia, I., Jimenez de Aberasturi, D., Pavlov, V., Sotomayor, M.D.P.T., Liz-Marzán, L.M., SERS-based immunoassay for monitoring cortisol-related disorders, *Biosensors and Bioelectronics* (2020), doi: https://doi.org/10.1016/j.bios.2020.112418.

CRediT author statement

Javier E.L. Villa: Conceptualization, Methodology, Formal Analysis, Writing-Editing **Isabel García:** Methodology, Writing-Reviewing **Dorleta Jimenez de Aberasturi:** Methodology, Writing-Reviewing **Valeri Pavlov:** Methodology, Writing-Reviewing **Maria D.P.T. Sotomayor:** Conceptualization, Writing-Reviewing **Luis M. Liz-Marzán:** Conceptualization, Methodology, Writing-Reviewing, Project Administration

Graphical Abstract

Rational design of a surface-enhanced Raman spectroscopy-based biosensor to monitor cortisol in biological fluids.

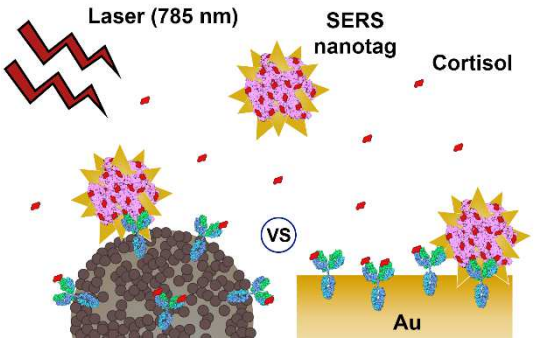

SERS-based immunoassay for monitoring cortisol-related disorders

Javier E.L. Villa[1,4,*], Isabel Garcia[1,2], Dorleta Jimenez de Aberasturi[1,2,3], Valeri Pavlov[1], Maria D.P.T. Sotomayor[4], Luis M. Liz-Marzán[1,2,3,*]

[1] CIC biomaGUNE, Basque Research and Technology Alliance (BRTA), Paseo de Miramón 182, 20014, Donostia-San Sebastián, Spain

[2] Centro de Investigación Biomédica en Red, Bioingeniería, Biomateriales y Nanomedicina (CIBER-BBN), Paseo de Miramón 182, 20014, Donostia-San Sebastián, Spain

[3] Ikerbasque, Basque Foundation for Science, 48013 Bilbao, Spain

[4] Instituto de Química and INCT-DATREM, Universidade Estadual Paulista (UNESP), Araraquara, CEP 14800-060, São Paulo, Brazil

* E-mail addresses of corresponding authors: villa.javier03@gmail.com (JELV); llizmarzan@cicbiomagune.es (LMLM)

Abstract

As a natural response to a stressful situation, the human body produces cortisol. For this reason, cortisol is also called “the stress hormone” and is considered to be the principal stress biomarker. Although cortisol response to stress is essential for survival, abnormal levels in biological fluids may represent serious health risks. In this work, we present a cortisol biosensor which relies on a highly sensitive technique (surface-enhanced Raman spectroscopy, SERS) and a specific recognition (immunoassay). Gold nanostars were used as SERS nanotags, since they provide a better response than nanorods or nanospheres. Using the same concept, two different immunoassay modalities were evaluated, using either magnetic beads or gold-coated glass slides decorated with cortisol antibodies, as the capture substrates. The magnetically-assisted SERS immunoassay presented a better performance and was therefore selected to quantify cortisol content in biological fluids (urine and serum). Significant advantages of this assay were found over standard methods such as Ultra Performance Liquid Chromatography-Mass Spectrometry (UPLC-MS) and Enzyme-Linked Immunosorbent Assay (ELISA), including higher sensitivity and repeatability, minimum sample preparation, simplicity, and portability. Therefore, the proposed SERS immunoassay might be implemented as a highly efficient tool for in situ monitoring of human stress levels and cortisol-related disorders (e.g. Cushing’s syndrome and Addison’s disease).

Keywords: Hydrocortisone, Surface-enhanced Raman spectroscopy, Plasmonics, Magnetic separation, UPLC-MS, ELISA.

1. Introduction

The need for protecting ourselves against predators and other aggressors used to be the main cause of stress. However, nowadays, we face a wider variety of stressful situations, including job dissatisfaction (huge workload, dangerous working conditions, competition, risk of job loss, etc.) and life stresses (financial obligations, emotional problems, pandemic lockdown, etc.) (Khalatbari et al., 2013; Slavich, 2016). Under high-stress lifestyle conditions, the human body reacts by constantly producing cortisol, which is considered to be the main stress biomarker (Holsboer and Ising, 2010). The abnormal increase in cortisol levels leads to depression of the immune system and increases fatty acid and amino acid concentrations in blood, which may contribute to the development of Cushing's syndrome, with symptoms including hypertension, obesity, depression and low bone mass (Nieman, 2015). On the other hand, an abnormal decrease in cortisol levels occurs when the adrenal glands are chronically fatigued, depleted and unable to meet the demands of the body. This condition has been reported in overweight and obese children (Kjölhede et al., 2014), as well as in people with Addison's disease, in which antibodies attack the adrenal cortex and is manifested by dizziness, fatigue, weight loss and darkening of skin folds and scars (Saevik et al., 2018). Thus, routine monitoring of cortisol levels is a crucial task for human well-being and early disease diagnosis.

To diagnose and treat cortisol-related conditions accurately, a regular evaluation of cortisol concentration in biological fluids is required. Since the physiologically relevant concentrations are very low (in the order of ng/mL) and biological fluids have complex matrices, cortisol monitoring remains a significant analytical challenge (Gatti et al., 2009; Kaushik et al., 2014). Currently, the most of efficient and well-established methods for cortisol determination are primarily based on mass spectrometry and ELISA (Albar et al., 2013; Gatti et al., 2009; Sturmer et al., 2018). Although these methods have good sensitivity and selectivity, they are laborious, time-consuming and hard to implement for

point-of-care testing. Such a personalized healthcare demands a rapid, portable, cost-effective and disposable sensor with low power consumption and low turnaround time (Kaushik et al., 2014). In this context, the combination of a highly sensitive and versatile technique (surface-enhanced Raman spectroscopy, SERS) and a highly selective assay (immunoassay) arises as an interesting alternative to fulfill these requirements.

SERS is a powerful spectroscopic technique that relies on a dramatic increase of the Raman scattering efficiency from molecules located in the vicinity of a nanostructured metallic surface (Langer et al., 2020; Stiles et al., 2008). Such an enhancement stems from a combination of electromagnetic (related to localized surface plasmon resonances, LSPR) and chemical (related to molecular polarizability) mechanisms (Morton and Jensen, 2009; Stiles et al., 2008), being the electromagnetic contribution the most prominent one. In virtue of its high sensitivity, SERS has been used for the detection of a wide variety of analytes, with sensitivity down to the single-molecule regime (Stiles et al., 2008). Nevertheless, the main limitation of SERS in this context is probably the poor capacity to selectively adsorb/approximate the analyte in the presence of potential interferences (molecules with similar or higher affinity for the nanostructured surface). To promote a selective approximation of the analyte to the nanosurface, strategies such as surface modification with capture agents and coupling with separation techniques, have been proposed (Sharma et al., 2016; Subaihi et al., 2017). Particularly, the use of antibodies as capture agents to perform SERS immunoassays (SERSIs) enables specific and sensitive analyte recognition, even in the presence of interferences (Smolsky et al., 2017). Although this strategy has been mainly applied to protein sensing at very low concentrations, some studies indicated that it might be extended to the detection of small molecules (Caglayan et al., 2017; Pei et al., 2013; Song et al., 2009; Wang et al., 2016). To achieve such a high sensitivity, most of the SERSIs promote the formation of nanoparticle clusters/aggregates to generate hotspots (inter-particle regions with strong electric fields), thereby maximizing

the SERS response. However, uncontrolled aggregation might lead to variable and non-reproducible results. Therefore, it is still challenging to achieve sensitive measurements from SERS nanotags under non-aggregating, controllable and more reproducible conditions. Furthermore, since the choice of the capture substrate (element that binds SERS nanotags) might have a significant influence on the sensitivity and reproducibility of the SERSI (Smolsky et al., 2017), it is also worth comparing the performance of different capture substrates.

We developed a sensitive and highly selective SERSI to quantify cortisol in biological fluids. Under non-aggregating conditions, gold nanostars, nanorods or nanospheres were assessed as SERS nanotags to achieve high sensitivity. Magnetic beads and gold-coated glass slides, functionalized with cortisol antibodies, were compared as capture substrates to perform an efficient immunoassay. The proposed SERSI displays significant advantages, in terms of speed, simplicity, repeatability and sensitivity, over both UPLC-MS and ELISA, toward the analysis of biological fluids containing cortisol at physiological concentrations. Thus, the proposed method is proposed as an efficient and reliable tool for monitoring stress and cortisol-related disorders.

2. Experimental section

2.1. Instrumentation

SERS spectra were collected with a confocal Raman microscope (Renishaw inVia) equipped with a 1024 x 512 CCD detector, using 532, 633 or 785 nm laser excitation sources. Under optimized conditions, we used excitation at 785 nm using a 10X objective with an integration time of 20 s, at a laser power of 90 mW. A portable Raman spectrometer iRaman (B&W Tek) with a 785 nm laser excitation source, an integration time of 6 s and a laser power of 100 mW, was also used. UPLC-MS measurements were performed using a UPLC Acquity (column C18, 100 x 2.1 mm – 1.7 µm) coupled to a LCT

Premier XE Time-of-Flight mass spectrometer (Waters) with a source of electrospray positive mode.

Transmission electron microscopy (TEM) images were collected with a JEOL JM-1400 PLUS TEM operating at 120 kV, using carbon-coated 400 square mesh copper grids. For scanning electron microscopy (SEM), a microscope FEI Helios NanoLab^{TM} 450S was used, operating at an accelerate voltage of 5 kV. UV-Vis extinction spectra were obtained using an Agilent 8453 UV-Vis diode array spectrophotometer. A 3D printer RegenHU (3D Discovery evolution) was used to print the silicone wells (5 mm diameter, 5 mm height). An AJA Magnetron sputtering system ATC 1800 UHV was used to deposit gold over glass slides. The base pressure in the chamber was 10^{-8} mTorr and plasma cleaning was performed for 10 minutes in RF Mode at a working pressure of 30 mTorr. Targets were Ti (99.995 %) from Kurt Lesker and Au (99.99 %) from AJA.

2.2. Chemicals

Deionized Milli-Q water (resistivity 18 MΩ·cm) was used for all solutions and standards. Hydrogen tetrachloroaurate trihydrate ($HAuCl_4 \cdot 3H_2O$, ≥99.9 %), sodium citrate tribasic dihydrate (≥98 %), silver nitrate ($AgNO_3$, >99 %), L-ascorbic acid (AA, >99 %), poly(ethylene glycol) 2-mercaptoethylether acetic acid (HS-PEG-COOH, MW 5000 g/mol), 2-(N-morpholino)ethanesulfonic acid (MES, ≥99.5 %), 4-mercaptobenzoic acid (MBA, ≥98 %), 1-ethyl-3-(3-dimethylaminopropyl) carbodiimide (EDC, ≥99%), N-hydroxysuccinimide (NHS, 98 %), bovine serum albumin (BSA, ≥98 %), phosphate buffer solution (PBS, 100 mM), cetyltrimethylammonium bromide (CTAB, ≥98 %), *n*-decanol (≥98 %), hydrochloric acid (37 %), Ammonia solution (25 %), ethanol (≥99.8 %), acetonitrile (≥99.9 %), chloroform (≥99.8 %) and BCA protein assay kit were purchased from Sigma-Aldrich. 3,3'-dithiobis[6-nitrobenzoic acid]bis(succinimide)ester (DSNB) was purchased from Biosynth. Monoclonal cortisol antibody (1 mg/mL) and magnetic beads suspension (~800 nm

diameter, 50 mg/mL) with carboxylic functional groups were purchased from ThermoFisher; 1.8 mg/mL cortisol-BSA conjugate solution was purchased from Fitzgerald industries. All glassware was washed with aqua regia, rinsed at least three times with deionized water and dried before use.

2.3. SERS nanotags synthesis

2.3.1. Nanostars (GNSs)

GNSs were synthesized through surfactant–free method (De Silva Indrasekara et al., 2018) with modifications, which facilitate surface functionalization. Briefly, 20 µL of 0.128 M $HAuCl_4$ and 20 µL of 1 M HCl were added to 10 mL of deionized water under moderate stirring. After 1 min, from 20 to 160 µL of 2.9 x 10^{12} NPs/mL 15 nm gold seeds ([Au^0] = 0.5 mM, $Extinction_{400nm}$ = 1.2) (Scarabelli et al., 2015), prepared by citrate reduction, was added. After 20 s, with a delay of 5 s between them, 100 µL of 0.5 - 12 mM $AgNO_3$ and 100 µL of 50 mM AA was added. The solution turned bluish or dark green (depending on seed amount and $AgNO_3$ concentration), indicating GNSs formation. The reaction was allowed to proceed for 3 min and 100 µL of 1 mM HS-PEG-COOH was then added under vigorous stirring for 15 min. Thereafter, 20 µL of 10 mM Raman reporter (MBA) and 10 µL of 15 % v/v ammonia were added and stirring was maintained for 30 min. Finally, stirring was interrupted and GNSs were washed by centrifugation (1,192 g, 10 min) to remove excess reagents.

To obtain SERS nanotags from GNSs, the carboxylic groups were activated via EDC/NHS reaction. 10 µL of 10 mM EDC and 15 µL of 10 mM NHS were mixed and added to 2 mL of GNS ($Extinction_{400nm}$ = 1.0) under shaking for 30 minutes. The particles were then washed by centrifugation (1,192 g, 10 min) to remove excess reagents and resuspended in 10 mM MES (pH 6). Thereafter, 10 µL of cortisol-BSA conjugate (1.8 mg/mL) was added and the reaction was shaken for 2 hours. Finally, 10 µL of 20 mg/mL

BSA was added to block bare sites and the reaction was shaken for 1 h. The resulting solution was washed twice by centrifugation (1,192 g, 10 min) and resuspended in 10 mM PBS (pH 7.2).

2.3.2. Nanorods (GNRs)

GNRs (60 nm length, 15 nm width), with a main LSPR near 785 nm (longitudinal mode) and another at 509 nm (transverse mode), were synthesized via a recently reported protocol (González-Rubio et al., 2019), then washed by centrifugation (6,225 g, 20 min) and resuspended in water. Then, 10 µL of 1 mM HS-PEG-COOH was added to 2 mL of GNR ($Extinction_{400nm}$ = 1.0) under rapid stirring for 1 h. The amount of HS-PEG-COOH to be added was selected to avoid any change in the extinction spectrum (which would indicate aggregation), due to replacement of CTAB by MBA molecules. Finally, 20 µL of 10 mM MBA was added under stirring for 6 h and the solution was then washed by centrifugation (6,225 g, 20 min). The amount of MBA was selected to maximize the SERS signal from GNR nanotags.

2.3.3. Nanospheres (GNPs)

GNPs (46 nm diameter) with LSPR near 532 nm, were synthesized following a seeded growth method (Bastús et al., 2011). In short, 150 mL of 2.2 mM sodium citrate was heated to boiling and 1 mL of 25 mM $HAuCl_4$ was then added under vigorous stirring. After 10 min, the solution was cooled down to 90 ºC and 1 mL of 25 mM $HAuCl_4$ was then added. After 30 min, 1 mL of 25 mM $HAuCl_4$ was added and the reaction was continued for 30 min. A 55 mL aliquot was extracted and 53 mL of water and 2 mL of 60 mM sodium citrate were added. The resulting solution was used as a new seed solution and the process was repeated four times. Thereafter, 10 µL of 1 mM HS-PEG-COOH was added to 2 mL of the GNP solution ($Extinction_{400nm}$ = 1.0) under strong stirring for 15 min. Finally,

20 µL of 10 mM MBA was added under stirring for 30 min and the solution was washed by centrifugation. The amounts of HS-PEG-COOH and MBA were selected to maximize the SERS signal and guarantee the stability of GNSs.

2.4. Preparation of capture substrates

2.4.1. Magnetic beads (MBs) decorated with cortisol antibodies

A magnetically separable capture substrate was prepared using a suspension of MBs carrying carboxylic functional groups. Briefly, 200 µL of 50 mg/mL MBs was washed using a magnet for MB concentration and resuspended in 500 µL of 10 mM MES buffer at pH 6. The carboxylic groups were then modified via EDC/NHS reaction, in which 250 µL of 20 mg/mL EDC and 250 µL of 25 mg/mL NHS were added to the MB suspension and shaken for 30 min. The particles were then magnetically separated and washed twice with 10 mM MES buffer (pH 6.0). Then, 50 µL of 1 mg/mL monoclonal cortisol antibody was added and the reaction mixture was shaken for 2 h. Finally, 50 µL of 20 mg/mL BSA was added to block bare sites and shaking was continued for 1 h. To remove excess reagents, the magnetic capture substrate was washed twice and resuspended in 1 mL of 10 mM PBS buffer (pH 7.2).

2.4.2. Gold-coated glass (GCG) decorated with cortisol antibodies

To fabricate rigid capture substrates, glass slides (26 mm x 76 mm) were covered with a 200 nm gold layer by sputtering under Ar gas flow (24 cm^3/min) at room temperature, with a rotating platform to improve deposition uniformity. A 6 nm Ti layer was applied before gold deposition to improve adhesion. Silicone wells of 5 mm diameter and 5 mm height were then 3D printed onto the GCG substrates. The gold active area from each well was individually modified with 20 µL of 0.1 mM DNSB in acetonitrile under shaking for 3 h. The wells were then washed twice with acetonitrile and once with water, to remove

excess DSNB. Thereafter, 20 µL of 0.05 mg/mL cortisol monoclonal antibody in PBS pH 7.2 was added to each well and shaken for 4 h. Finally, 20 µL of 1 mg/mL BSA was added to block bare sites and the reaction was shaken for 1 h and washed three-fold with deionized water.

2.5. SERS immunoassay (SERSI) modalities

2.5.1. Magnetically-assisted SERS immunoassay (MA-SERSI)

MA-SERSI was carried out by mixing three different solutions: (1) SERS nanotags (GNSs functionalized with MBA molecules and cortisol-BSA conjugates), (2) magnetically separable capture substrate (MBs decorated with cortisol antibodies), and (3) sample (with or without free cortisol). The capture substrate suspension, the sample and the SERS nanotags were added sequentially in that order. The volumes of each solution were fixed to 200 µL, thereby minimizing the possibility of competition between adsorption and diffusion. The SERS nanotags/MBs ratio was selected by identifying the minimum amount of capture substrate required to bind all SERS nanotags from the colloid. The mixture of all three components was incubated for 2 h under gentle shaking and the capture substrate suspension was then separated magnetically. Finally, the SERS signal was recorded from the supernatant.

2.5.2. Rigid substrate SERS immunoassay (RS-SERSI)

For RS-SERSI, 15 µL of sample and 15 µL of SERS nanotags were sequentially poured into the wells and shaken for 3 h. During this time, the rigid capture agent binds both SERS nanotags and free cortisol from the solution. Thereafter, the solution was discarded and the wells were washed four times with deionized water. The active area containing captured SERS nanotags and cortisol was dried and the SERS signal collected.

2.6. Biological fluid samples

Two different biological fluids were analyzed, urine and serum. The urine sample was a commercially available (Sigma-Aldrich) standard human urine simulant. Real serum samples, including a serum certified reference material (CRM), purchased from Sigma-Aldrich, were also analyzed. In all cases, the samples were simply diluted to 50% in deionized water prior to analysis.

2.7. Reference methods

To validate SERSI results, the samples were also analyzed by two well-stablished analytical techniques, UPLC-MS and ELISA. For UPLC-MS, all standards and samples were prepared following a protein precipitation procedure. Cortisol was extracted from the samples after protein precipitation with an equal volume of 5% trifluoroacetic acid in acetonitrile. The mixture was shaken for 2 h and the samples were then centrifuged at 9,727 g for 10 min. 10 µL of the supernatant was collected and injected. The mobile phase comprised 0.1% formic acid and methanol at a flow rate of 300 µL/min. Examples of chromatogram and mass spectrum of a cortisol sample are shown in Fig. S1. A commercially available Cortisol Competitive Human ELISA kit (EIAHCOR, 96 tests) for cortisol determination was purchased from Thermo Fisher Scientific and used following the kit protocol.

3. Results and discussion

We implemented two different SERSI platforms, in which the same SERS nanotags and antibodies but different substrates were employed. In both cases, we monitored changes in the SERS intensity from nanotags, as a function of cortisol concentration in the sample. A schematic representation of both modalities is presented in Fig.1. In the MA-SERSI procedure (Fig. 1a) the capture substrate (MBs decorated with cortisol antibodies)

would bind both SERS nanotags (via antibody-cortisol-BSA) but also free cortisol, prior to magnetic separation. As a result, the SERS signal would be recorded from non-captured SERS nanotags remaining as a colloidal dispersion, which should increase for a higher concentration of free cortisol in the sample. On the other hand, for a cortisol-free sample, the capture substrate would bind all SERS nanotags, so that the SERS signal from the colloidal solution will be close to zero after magnetic removal of MBs. On the other hand, the RS-SERSI mechanism makes use of GCG decorated with cortisol antibodies as the capture substrate (Fig. 1b). Because SERS is now recorded from the capture substrate (Au-sputtered glass slide), not from the supernatant, the SERS signal should decrease for increasing cortisol concentrations. In other words, the response collected from the rigid capture substrate would be maximum in the absence of free cortisol (more SERS nanotags captured) and minimum under excess of free cortisol (less nanotags captured).

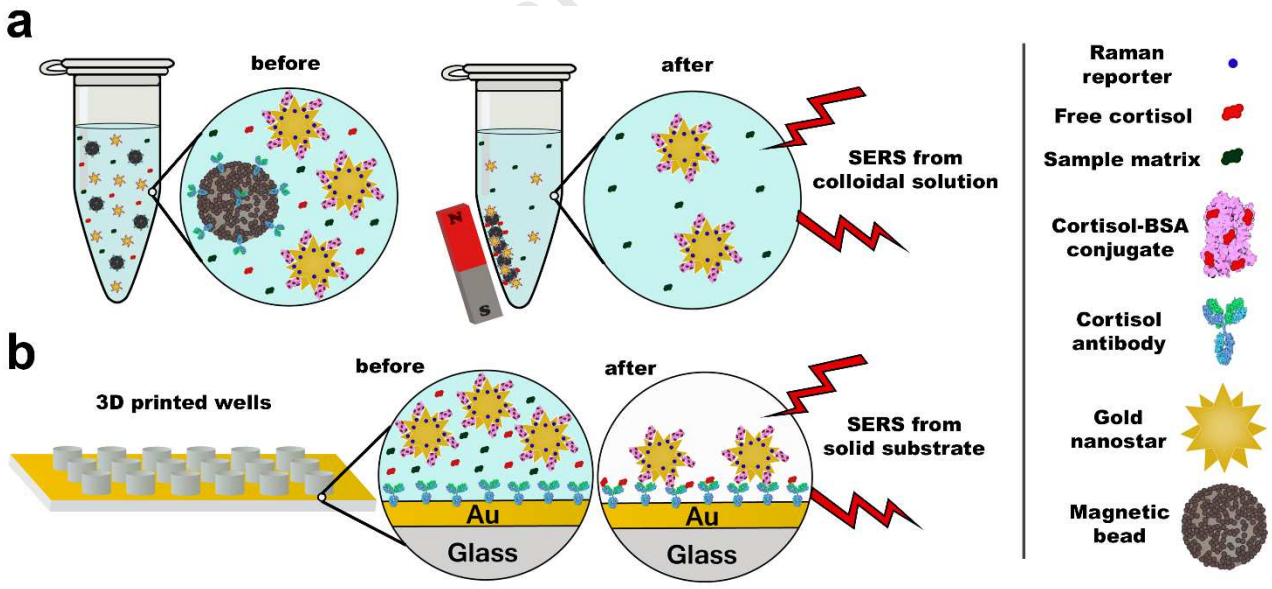

Fig. 1. Description of SERSI modalities. (a) MA-SERSI, using a suspension of magnetic beads decorated with cortisol antibodies as capture substrate; (b) RS-SERSI, using gold-coated glass decorated with cortisol antibodies as capture substrate. SERS nanotags comprise gold nanostars functionalized with Raman reporter molecules and cortisol-BSA conjugates that selectively bind to cortisol-specific antibodies.

3.1. SERS nanotags optimization

The signal provided by SERS nanotags is a key parameter that determines the sensitivity of a SERSI method. Accordingly, the performances of gold nanoparticles with different shapes (GNSs, GNRs and GNPs) were assessed. For GNSs under non-aggregating conditions, a maximum SERS signal should be achieved when the LSPR closely matches the Raman laser excitation wavelength at 785 nm. We thus carried out GNS synthesis under various conditions, to tune the LSPR around 785 nm. Shown in Fig. S2 are the extinction and SERS spectra for GNSs obtained by varying $AgNO_3$ concentration and amount of seeds. The corresponding effects on GNS morphology are shown in Figs. S3 and S4. According to these results, a compromise was found to maximize the SERS signal while preserving the GNS shape, when using 100 µL of 6 mM $AgNO_3$ and 80 µL of 2.9×10^{12} NPs/mL seed solution ($Extinction_{400nm}$ = 1.2).

After establishing the synthesis conditions for GNSs, their SERS performance was compared to those obtained using GNRs and GNPs (which are recurrently used in SERS sensing applications). The syntheses of GNRs and GNPs were tuned to obtain LSPRs near laser excitations at 785 nm and 532 nm, respectively. Representative TEM images from GNSs, GNRs and GNPs, synthesized under optimized conditions, are provided in Figs. 2 and S5. Fig. 2a also displays the extinction spectra to identify the LSPR maxima, as well as the wavelengths of the three Raman laser excitations tested. Accordingly, 785 nm laser excitation should be used for GNSs and GNRs, whereas 532 nm laser excitation should work best for GNPs. The results are summarized in Fig. 2b, showing the strongest signals for GNSs and GNRs when using 785 nm laser excitation, as expected. The superior performance of GNSs as compared to GNRs is likely due to their different morphologies. As GNS contain numerous sharp tips, multiple hotspots can be generated in every GNS; in contrast, only two hotspots (at the tips) are generated in one GNR. On

the other hand, it can also be observed in Fig. 2b that the strongest signal for GNPs was achieved by using 633 nm laser excitation, because of hotspots generated in the gaps of few dimers or trimers coexisting with individual GNPs in solution. It has been previously demonstrated that such small GNPs clusters display a strong LSPR around 633 nm (Fraire et al., 2013; Wustholz et al., 2010) and high signal at an excitation wavelength different to that expected for GNP monomers (532 nm) can be experimentally obtained (Álvarez-Puebla, 2012). However, the signal provided by GNPs at 633 nm was still lower than that from GNSs, and depends on the gap distance and number of particles per cluster formed, parameters which are hard to control. Therefore, we selected GNSs as SERS nanotags for further experiments, aiming to highly sensitive and reproducible SERS cortisol detection. The SERS signal from these nanotags was monitored for 1 month and no significant changes were observed, thus indicating that SERS nanotags were highly stable and resistant to photodamage under the selected instrumental conditions.

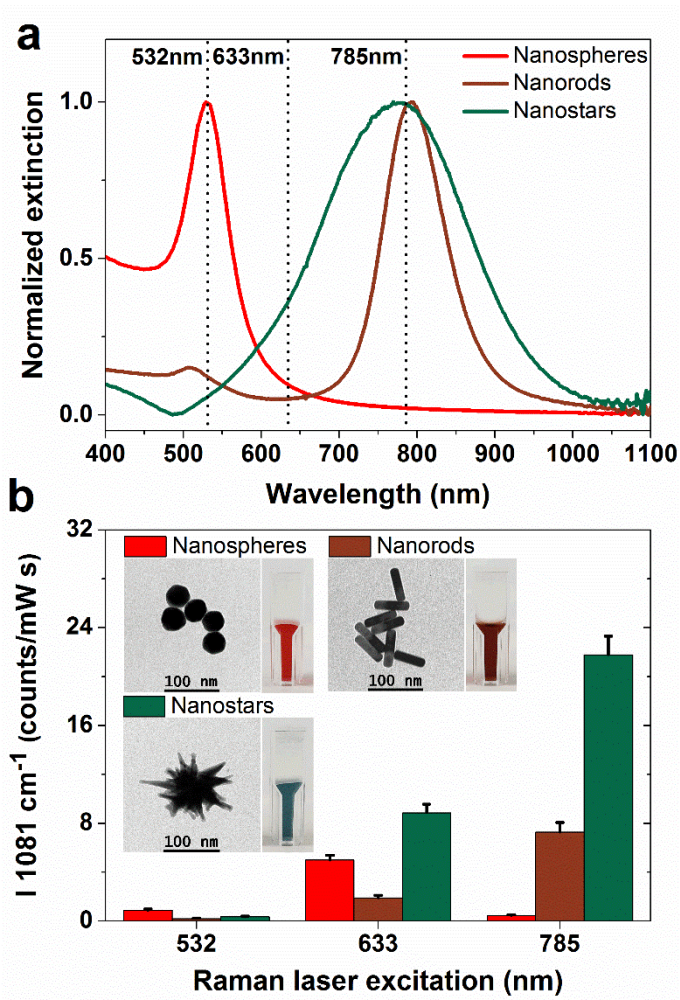

Fig. 2. Comparison of extinction spectra (a) and SERS signals at 1081 cm^{-1} (b), from differently shaped nanotags (GNSs, GNRs, GNPs). The concentrations were fixed at [Au^0] = 0.25 mM ($Extinction_{400nm}$ = 0.6), for SERS signal comparison, and these values were normalized by the corresponding laser excitation power.

3.2. Capture substrates and SERSI comparison

Since the capture substrate plays the role of binding SERS nanotags, we expected that their mutual interaction should influence the SERSI performance. For example, analysis time and sensitivity might be affected if the immunoassay is carried out using either a suspension or a rigid capture substrate (Smolsky et al., 2017). Therefore, identification of the advantages and limitations provided by each capture substrate is a key step toward developing an efficient SERSI method. As shown in Fig. 1, we explored two

different immunoassay modalities: MA-SERSI and RS-SERSI. For MA-SERSI, a suspension of MBs decorated with cortisol antibodies was used as the capture substrate. A preliminary study was carried out to stablish the suitable pH value and EDC/MBs concentration ratio to prepare the magnetic capture substrate (Fig. 3a). A pH value of 6 and 250 µL of EDC (20 mg/mL) per 200 µL of MBs (50 mg/mL) were ultimately selected. These conditions allowed us to maximize the binding of cortisol antibodies to MBs (indirectly measured by total protein quantification of the supernatant) via EDC/NHS reaction, while preserving the antibody activity, which might be affected at lower pH values. The interaction of the magnetic capture substrate with SERS nanotags was also assessed by TEM (Fig. 3b). TEM images were obtained after mixing and washing MBs, decorated and not decorated with cortisol antibodies, with SERS nanotags. The results show that the capture substrate can efficiently bind SERS nanotags via interactions between cortisol antibody and cortisol-BSA conjugate. Therefore, cortisol antibodies were successfully bound to MBs, yielding a magnetic capture substrate that can bind cortisol-BSA conjugates at the SERS nanotags surface.

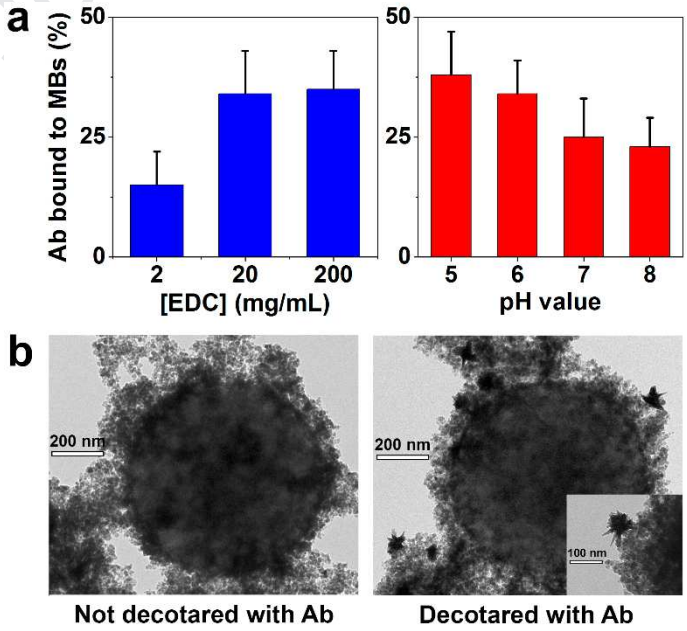

Fig. 3. (a) Effect of EDC concentration and pH on the efficiency of cortisol antibody binding to MBs. The amount of cortisol antibodies was determined using a commercially available BCA protein quantification kit. (b) Representative TEM images of MBs, not decorated (left) and decorated (right) with cortisol antibodies, after interacting with SERS nanotags.

The SERS signals recorded after performing the MA-SERSI for different cortisol concentrations were evaluated, as shown in Fig. 4a. We hypothesized that an increase in cortisol concentration should lead to increased SERS signal from the supernatant, as a result of the competition between nanotags and free cortisol for binding sites on the MB capture substrate. This means that a high cortisol concentration would saturate the available binding sites before magnetic separation, leaving a high concentration of SERS nanotags in solution. As shown in Fig. 4a, the SERS signal did increase with cortisol concentration, up to a maximum corresponding to the initial SERS nanotags remaining in solution after magnetic separation. Since signal saturation was only observed for high cortisol concentrations, we used the linear range at lower concentrations for cortisol quantification at physiological levels. For example, normal cortisol concentration ranges from 10 to 100 ng/mL in urine, and from 20 to 250 ng/mL in serum (Kaushik et al., 2014). The linearity of the plot was tested by analysis of variance (ANOVA) and indicated no significant deviation from linearity ($p < 0.05$) in the range between 12.5 and 400 ng/mL. The relative standard deviations of SERS signals ranged between 8% (high cortisol levels) and 16% (low cortisol levels), which can be considered as reproducible values for cortisol quantification in biological fluids (Gatti et al., 2009). We propose that a key element was related to avoiding uncontrolled formation of GNS aggregates/clusters, so that the measurements were performed under controlled conditions.

To evaluate the selectivity of the capture system, MA-SERSI was individually tested for cortisol and some of the potential interferences that can be found in biological fluids,

such as hormones with similar chemical structures (see Fig. 4b). According to the detection mechanism, the presence of a hormones other than cortisol should result in low SERS signals, because the capture agent would bind and remove SERS nanotags only from the mixture. The results are summarized in Fig. 4b, indeed showing the highest SERS signal for cortisol, much lower signals for other hormones at the same concentration. No significance difference (95% of confidence level) was observed between the SERS signal for cortisol (200 ng/mL) and mixtures of cortisol (200 ng/mL) and other hormones (100 ng/mL). These results demonstrate that the antibodies linked to MBs are capable of capturing both SERS nanotags and free cortisol, but not hormones with cortisol-like structure. We can thus confirm that cortisol monoclonal antibodies on the capture substrates provide excellent selectivity, which is a key toward the analysis of samples within complex matrices (e.g. biological fluids).

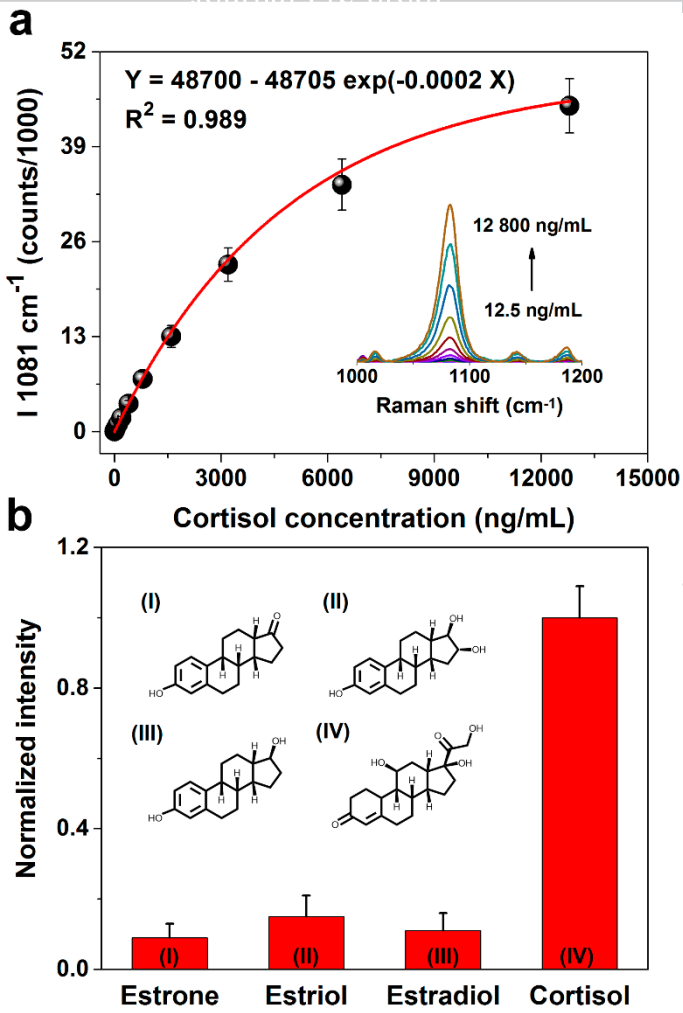

Fig. 4. (a) Influence of cortisol concentration on SERS signal in MA-SERSI. (b) Selectivity of MA-SERSI, analyzed as SERS intensity for different hormones: cortisol, estrone, estriol and estradiol. All concentrations were 200 ng/mL, the SERS signal was recorded at 1081 cm^{-1}. All experiments were performed in triplicate.

As cortisol levels in biological fluids might also change depending on the day-night cycle, the capacity to perform in situ measurements is important to provide personalized healthcare. We thus assessed the possibility of performing in situ cortisol determinations using a portable Raman spectrometer (Fig. S6). The instrumental conditions were different in terms of laser power and illumination time (see Experimental section 2.1) because of differences in laser focusing and laser power control, which are limited when using commercially available portable Raman spectrometers. This limitation hinders, for

example, measurements requiring the laser beam to be accurately focused on a rigid surface (i.e. RS-SERSI). However, we found that the performance of both Raman spectrometers was similar under the MA-SERSI modality, suggesting that the method can be readily implemented for point-of-care measurements.

In the RS-SERSI modality, cortisol antibodies were covalently linked to a GCG surface, used as the capture substrate (Fig. 5a). The use of 3D printed silicone wells on the gold surface allowed us to efficiently control the available active area, thereby minimizing the amount of reagents per assay. This feature represents a significant advantage when routine and high demand assays are required (i.e. it becomes a cost-effective method). The affinity of the capture substrate for SERS nanotags was demonstrated by SEM imaging of the GCG surface after performing the RS-SERSI, as shown in Figs. 5b and 5c. Since the Raman signal was collected from the GCG surface after capturing SERS nanotags, the interaction between the SERS nanotags and the gold layer should generate additional hotspots, resulting in a stronger SERS signal. To test this hypothesis, we compared the SERS signals obtained from nanotags on GCG and on glass surfaces (Fig. S7). As expected, the signal obtained from SERS nanotags on the GCG surface was much higher than those obtained from either SERS nanotags on a glass surface or MBA molecules directly attached onto the GCG surface.

Comparison of both SERSI modalities was carried out by obtaining calibration curves for cortisol quantification under optimized conditions (Figs. 5d and 5e, for MA-SERSI and RS-SERSI respectively). It should be noted that the signs of the slopes are opposite because of the different modalities for collecting the signals, from remaining SERS nanotags in the MA mode but from the capture substrate in the RS mode. Figs. 5d and 5e also reveal a higher sensitivity for RS-SERSI, as provided by the slope of the calibration curve. The corresponding limits of detection (LODs, defined as $3s_y/s$, where s_y is the standard deviation of the blank sample and s the slope of the calibration curve) were

7 ng/mL and 3 ng/mL for MA-SERSI and RS-SERSI, respectively. Since both LODs are below the lower limit of normal cortisol levels in urine (10-100 ng/mL) and serum (20-250 ng/mL), we conclude that both methods are suitable to monitor human stress levels and cortisol-related disorders. It should be noted that not only a better precision and a wider linear range were obtained for MA-SERSI, but additionally it is faster, as the signal is directly collected from solution, avoiding time-consuming washing steps. The inferior precision of RS-SERSI is likely related to the dependence on new parameters of the system, such as the number of tips in GNSs and their separation distance to the gold layer. Taking such important advantages into consideration, the MA-SERSI method was selected for application in biological fluids. Notwithstanding, RS-SERSI may be a good option for analyzing samples with lower cortisol levels, even if with less precision.

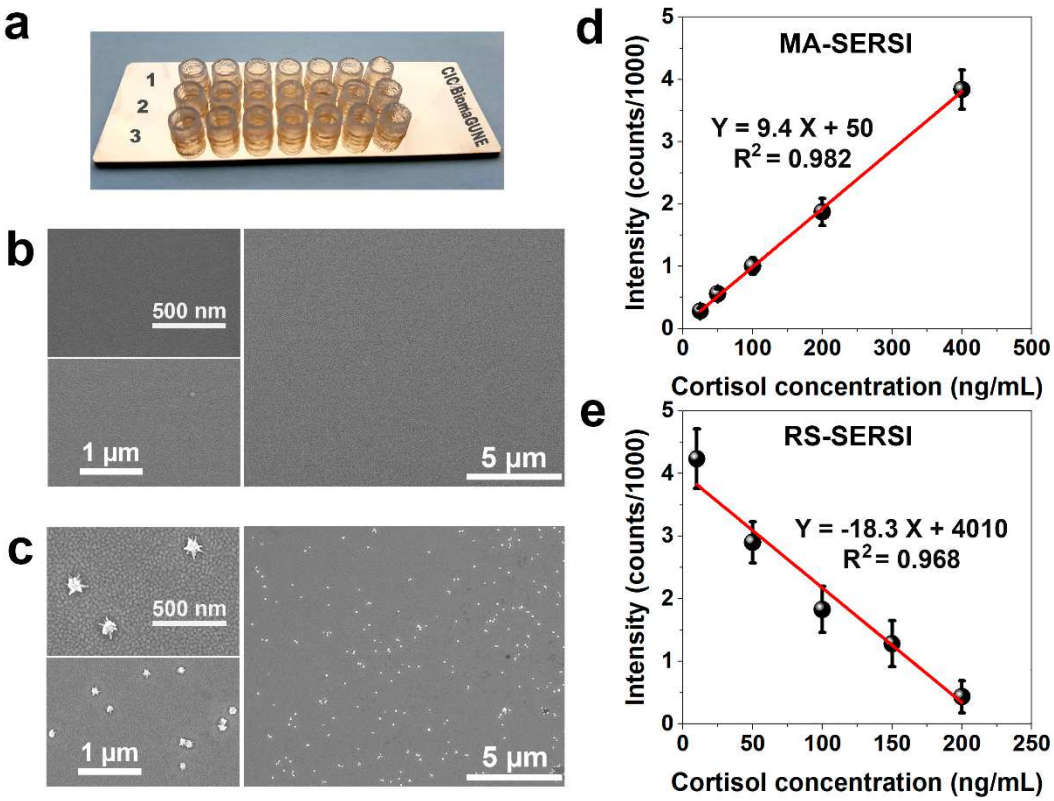

Fig. 5. (a) Photograph of a GCG substrate (26 x 76 mm) with 3D-printed wells. Representative high resolution SEM images of the GCG surface, non-decorated (b) and

decorated (c) with cortisol antibodies, after performing a RS-SERSI. (d, e) Comparison of calibration curves for cortisol determination using MA-SERSI (d) and RS-SERSI (e).

3.3. Analytical application and benchmarking

We finally demonstrate the suitability of the proposed MA-SERSI method to monitor cortisol in biological fluids, such as urine and serum. The accuracy and precision of the results were compared against two reference methods, UPLC-MS and ELISA, as summarized in Table 1. The corresponding calibration curves and cortisol quantification in the samples, measured by MA-SERSI, UPLC-MS and ELISA, are displayed in Fig. S8. These data indicate that the MA-SERSI method is suitable for quantification of cortisol in biological fluids, in a non-invasive fashion, at normal physiological concentrations and below. Compared to UPLC-MS, even though the accuracy and precision of MA-SERSI were similar, the need for extraction steps and use of organic solvents are avoided, significantly reducing analysis time and generation of residual solvents. On the other hand, when compared to ELISA, our method displayed better precision and limit of detection, thereby allowing the detection of lower cortisol concentrations. Thus, MA-SERSI features clear advantages over two of the most reliable analytical techniques for cortisol determination in biological fluids. Compared to other Raman spectroscopy (Gracie et al., 2017; Moore and Sharma, 2020) and immunoassay (de Ávila et al., 2017; Repetto et al., 2017) strategies for cortisol detection, our method displays a wider linear working range and superior sensitivity (particularly important for Adison's disease diagnosis) and reproducibility (no uncontrolled formation of aggregates/clusters). The MA-SERSI method might therefore be implemented toward in situ monitoring of human stress levels and cortisol-related disorders, such as Cushing's syndrome and Addison's disease.

Table 1. Comparison of actual and quantified cortisol concentrations in biological fluids using MA-SERSI, UPLC-MS and ELISA (n = 3).

Sample	Concentration spiked/certified*	Method		
		MA-SERSI*	ELISA*	UPLC-MS*
Serum	50	42 ± 9	61 ± 28	46 ± 8
	200	192 ± 21	189 ± 25	203 ± 17
Urine simulant	20	24 ± 8	<LOD	23 ± 6
	100	97 ± 16	109 ± 21	106 ± 15
Serum CRM	277 ± 5	270 ± 29	243 ± 34	263 ± 23

***** concentrations in ng/mL

4. Conclusions

We have successfully developed a novel SERS-based immunoassay for cortisol sensing in biological fluids. Under non-aggregating conditions, gold nanostars exhibit a greater SERS response than nanorods and nanospheres, and were thus used as SERS nanotags. Although gold-coated glass substrates provided an extra gain in sensitivity due to plasmon coupling with SERS nanotags, the magnetically separable capture substrate allowed performing a faster and more reproducible immunoassay, within a wider linear range. The proposed method proved suitable for cortisol determination at physiologically relevant concentrations, potentially becoming a reliable diagnostic tool. MA-SERSI presents significant advantages over well-stablished analytical techniques, UPLC-MS and ELISA, in terms of sample preparation, simplicity, portability, sensitivity and repeatability. This efficient method for cortisol sensing may be readily implemented for remote monitoring and diagnosis of stress and related disorders.

Supporting information

Additional information as noted in the text. UPLC-MS data, UV-Vis and SERS spectra, TEM and EDX images, additional calibration curves.

Notes

The authors declare no competing financial interests.

Acknowledgments

The authors would like to thank the Fundação de Amparo à Pesquisa do Estado de São Paulo (FAPESP – Grant No. 2018/24202-5 and 2014/50945-4) for the financial support. Funding by the European Research Council (ERC-AdG 4D-bioSERS, 787510) and the Spanish State Research Agency (Grants MAT2017-86659-R and BIO2017-88030-R) are gratefully acknowledged. This work was performed under the Maria de Maeztu Units of Excellence Program from the Spanish State Research Agency – Grant No. MDM-2017-0720. The authors thank Dr. Ana Sánchez Iglesias and Dr. Christian Kuttner for valuable advice regarding colloidal synthesis.

References

Albar, W.F., Russell, E.W., Koren, G., Rieder, M.J., Van Umm, S.H., 2013. Clin. Investig. Med. 36, 312–316.

Álvarez-Puebla, R.A., 2012. J. Phys. Chem. Lett. 3, 857–866.

Bastús, N.G., Comenge, J., Puntes, V., 2011. Langmuir 27, 11098–11105.

Caglayan, M.G., Kasap, E., Cetin, D., Suludere, Z., Tamer, U., 2017. Microchim. Acta 184, 1059–1067.

de Ávila, B.E.-F., Zhao, M., Campuzano, S., Ricci, F., Pingarrón, J.M., Mascini, M., Wang, J., 2017. Talanta 167, 651–657.

Indrasekara, A.S. de S., Johnson, S.F., Odion, R.A., Vo-Dinh, T., 2018. ACS Omega 3, 2202–2210.

Fraire, J.C., Pérez, L.A., Coronado, E.A., 2013. J. Phys. Chem. C 117, 23090–23107.

Gatti, R., Antonelli, G., Prearo, M., Spinella, P., Cappellin, E., De Palo, E.F., 2009. Clin. Biochem. 42, 1205–1217.

González-Rubio, G., Kumar, V., Llombart, P., Díaz-Núñez, P., Bladt, E., Altantzis, T., Bals, S., Peña-Rodríguez, O., Noya, E.G., MacDowell, L.G., Guerrero-Martínez, A., Liz-Marzán, L.M., 2019. ACS Nano 13, 4424–4435.

Gracie, K., Pang, S., Jones, G.M., Faulds, K., Braybrook, J., Graham, D., 2017. Anal. Methods 9, 1589–1594.

Holsboer, F., Ising, M., 2010. Annu. Rev. Psychol. 61, 81–109.

Kaushik, A., Vasudev, A., Arya, S.K., Pasha, S.K., Bhansali, S., 2014. Biosens. Bioelectron. 53, 499–512.

Khalatbari, J., Ghorbanshiroudi, S., Firouzbakhsh, M., 2013. Procedia - Soc. Behav. Sci. 84, 860–863.

Kjölhede, E.A., Gustafsson, PE, Gustafsson, PA, Nelson, N., 2014. Acta Paediatr. 103, 295–299.

Langer, J., Jimenez de Aberasturi, D., Aizpurua, J., Alvarez-Puebla, R.A., Auguié, B., Baumberg, J.J., Bazan, G.C., Bell, S.E.J., Boisen, A., Brolo, A.G., Choo, J., Cialla-May, D., Deckert, V., Fabris, L., Faulds, K., García de Abajo, F.J., Goodacre, R., Graham, D., Haes, A.J., Haynes, C.L., Huck, C., Itoh, T., Käll, M., Kneipp, J., Kotov, N.A., Kuang, H., Le Ru, E.C., Lee, H.K., Li, J.-F., Ling, X.Y., Maier, S.A., Mayerhöfer, T., Moskovits, M., Murakoshi, K., Nam, J.-M., Nie, S., Ozaki, Y., Pastoriza-Santos, I., Perez-Juste, J., Popp, J., Pucci, A., Reich, S., Ren, B., Schatz, G.C., Shegai, T., Schlücker, S., Tay, L.-L., Thomas, K.G., Tian, Z.-Q., Van Duyne, R.P., Vo-Dinh, T., Wang, Y., Willets, K.A., Xu, C., Xu, H., Xu, Y., Yamamoto, Y.S., Zhao, B., Liz-Marzán,

L.M., 2020. ACS Nano 14, 28–117.

Moore, T.J., Sharma, B., 2020. Anal. Chem. 92, 2052–2057.

Morton, S.M., Jensen, L., 2009. J. Am. Chem. Soc. 131, 4090–4098.

Nieman, L.K., 2015. Eur. J. Endocrinol. 173, M33–M38.

Pei, Y., Wang, Z., Zong, S., Cui, Y., 2013. J. Mater. Chem. B 1, 3992–3998.

Repetto, E.M., Gonzalez, D., Jacobsen, D., Smithuis, F., Jamardo, J., Cano, M., Aranda, C., Oneto, A., Berg, G., Fabre, B., 2017. Clin. Chem. Lab. Med. 55, e65–e68.

Saevik, Å.B., Åkerman, A.-K., Grønning, K., Nermoen, I., Valland, S.F., Finnes, T.E., Isaksson, M., Dahlqvist, P., Bergthorsdottir, R., Ekwall, O., Skov, J., Nedrebø, B.G., Hulting, A.-L., Wahlberg, J., Svartberg, J., Höybye, C., Bleskestad, I.H., Jørgensen, A.P., Kämpe, O., Øksnes, M., Bensing, S., Husebye, E.S., 2018. J. Intern. Med. 283, 190–199.

Scarabelli, L., Sánchez-Iglesias, A., Pérez-Juste, J., Liz-Marzán, L.M., 2015. J. Phys. Chem. Lett. 6, 4270–4279.

Sharma, B., Bugga, P., Madison, L.R., Henry, A.I., Blaber, M.G., Greeneltch, N.G., Chiang, N., Mrksich, M., Schatz, G.C., Van Duyne, R.P., 2016. J. Am. Chem. Soc. 138, 13952–13959.

Slavich, G.M., 2016. Teach. Psychol. 43, 346–355.

Smolsky, J., Kaur, S., Hayashi, C., Batra, S., Krasnoslobodtsev, A., 2017. Biosensors 7, 7.

Song, C., Wang, Z., Zhang, R., Yang, J., Tan, X., Cui, Y., 2009. Biosens. Bioelectron. 25, 826–831.

Stiles, P.L., Dieringer, J.A., Shah, N.C., Van Duyne, R.P., 2008. Annu. Rev. Anal. Chem. 1, 601–626.

Sturmer, L.R., Dodd, D., Chao, C.S., Shi, R.-Z., 2018. Steroids 129, 35–40.

Subaihi, A., Trivedi, D.K., Hollywood, K.A., Bluett, J., Xu, Y., Muhamadali, H., Ellis, D.I., Goodacre, R., 2017. Anal. Chem. 89, 6702–6709.

Wang, R., Chon, H., Lee, S., Cheng, Z., Hong, S.H., Yoon, Y.H., Choo, J., 2016. ACS Appl. Mater. Interfaces 8, 10665–10672.

Wustholz, K.L., Henry, A.-I., McMahon, J.M., Freeman, R.G., Valley, N., Piotti, M.E., Natan, M.J., Schatz, G.C., Van Duyne, R.P., 2010. J. Am. Chem. Soc. 132, 10903–10910.

Highlights:

- A cortisol biosensor was developed, which relies on a highly sensitive technique (surface-enhanced Raman spectroscopy, SERS) and a specific recognition (immunoassay).
- Two immunoassay modalities were evaluated, using either magnetic beads or gold-coated glass slides decorated with cortisol antibodies, as the capture substrates.
- The magnetically-assisted SERS immunoassay presented an excellent performance and was therefore selected to quantify cortisol content in biological fluids (urine and serum).
- Advantages of this assay were found over standard methods such as Ultra Performance Liquid Chromatography-Mass Spectrometry (UPLC-MS) and Enzyme-Linked Immunosorbent Assay (ELISA)

Declaration of interests

☒ The authors declare that they have no known competing financial interests or personal relationships that could have appeared to influence the work reported in this paper.

☐The authors declare the following financial interests/personal relationships which may be considered as potential competing interests: